

AD-A259 517



## MENTATION PAGE

Form Approved  
OMB No. 0704-0188

Estimated to average 1 hour per response, including the time for reviewing instructions, searching existing data sources, gathering the collection of information, and reviewing the collection of information. Send comments regarding this burden estimate or any other aspect of this burden, to Washington Headquarters Services, Directorate for Information Operations and Reports, 1215 Jefferson Avenue, S.W., Washington, D.C. 20540, and to the Office of Management and Budget, Paperwork Reduction Project (0704-0188), Washington, DC 20503.

1. AGENCY USE ONLY (Leave blank)		2. REPORT DATE 16 Dec 1992		3. REPORT TYPE AND DATES COVERED Scientific Paper	
4. TITLE AND SUBTITLE "Water Regions Extraction From Radar Imagery Using A Neural Network"				5. FUNDING NUMBERS R-195 <span style="border: 1px solid black; border-radius: 50%; padding: 5px; display: inline-block; text-align: center;">2</span>	
6. AUTHOR(S) Tho Cong Tran and Dr. Pi-Fuay Chen					
7. PERFORMING ORGANIZATION NAME(S) AND ADDRESS(ES) U.S. Army Topographic Engineering Center ATTN: CETEC-LO Fort Belvoir, VA 22060-5546				8. PERFORMING ORGANIZATION REPORT NUMBER	
9. SPONSORING/MONITORING AGENCY NAME(S) AND ADDRESS(ES)				10. SPONSORING/MONITORING AGENCY REPORT NUMBER	
11. SUPPLEMENTARY NOTES					
12a. DISTRIBUTION/AVAILABILITY STATEMENT Approved for Public Release: Distribution is Unlimited.				12b. DISTRIBUTION CODE	
13. ABSTRACT (Maximum 200 words) An artificial neural network concept is explored and developed for detecting and extracting water regions from radar imagery. A backpropagation neural network consisting of three layers of processing elements (PEs) is selected for this application. The input layer is composed of nine PEs that are arranged to process a single pixel at the same time. Two PEs in a hidden layer are sufficient for delineating water from other terrain categories. A single output PE with a thresholding function classify effectively all test images into two terrain categories: water and non-water. Large-scale Synthetic Aperture Radar (SAR) images, containing 512 by 512 pixels, were used as the test images for this experiment. Two blocks of water regions totalling 2,048 pixels were extracted for training the network. All the water pixels were classified correctly, while more than 99 percent of the non-water pixels were correctly classified.					
14. SUBJECT TERMS Neural Networks, Pattern Classification, Machine Vision, Radar Imagery, Supervised Learning/KEY WORDS				15. NUMBER OF PAGES 4	
				16. PRICE CODE	
17. SECURITY CLASSIFICATION OF REPORT Unclassified	18. SECURITY CLASSIFICATION OF THIS PAGE Unclassified	19. SECURITY CLASSIFICATION OF ABSTRACT Unclassified	20. LIMITATION OF ABSTRACT		

# WATER REGIONS EXTRACTION FROM RADAR IMAGERY USING A NEURAL NETWORK

Tho Cong Tran and Pi-Fuay Chen  
U. S. Army Topographic Engineering Center  
Fort Belvoir, VA 22060-5546

## ABSTRACT

An artificial neural network concept is explored and developed for detecting and extracting water regions from radar imagery. A backpropagation neural network consisting of three layers of processing elements (PEs) is selected for this application. The input layer is composed of nine PEs that are arranged to process a single pixel at the same time. Two PEs in a hidden layer are sufficient for delineating water from other terrain categories. A single output PE with a thresholding function classify effectively all test images into two terrain categories: water and non-water. Large-scale Synthetic Aperture Radar (SAR) images, containing 512 by 512 pixels, were used as the test images for this experiment. Two blocks of water regions totalling 2,048 pixels were extracted for training the network. All the water pixels were classified correctly, while more than 99 percent of the non-water pixels were correctly classified.

## INTRODUCTION

The automatic detection and extraction of water regions from radar imagery have been a subject of research for some time. Various pattern classification methods dealing with segmentation, classification, and extraction of terrain categories such as water, forests, fields, and built-up areas have been reported [1]. Statistical pattern recognition, image processing, and computer vision algorithms were exclusively used in a conventional computer system to solve the above problem. Because of their single-channel data processing capability, most conventional computers are inherently slow. In addition, the majority of terrain classification software routines are very complicated and require an excessively long time to implement and run.

In this paper, an alternate technique is described for processing and classifying SAR imagery using an artificial neural network. Artificial neural networks, which attempt to model the functions and architectures of the human brain, are massively parallel and highly adaptive or trainable. This implies that they can be operated at a high speed and they are fault-tolerant. Thus, the selection of a neural network for processing and classifying large scale SAR imagery seems reasonable and justifiable. The following sections discuss in detail the implementation of a backpropagation neural network, the training processes and testing results for the network, and the conclusions for this research.

## IMPLEMENTATION OF THE NEURAL NETWORK

The water finding task described above is a pattern classification problem. It can be solved by using many neural network architectures such as backpropagation, ADALINE (Adaptive Linear Neuron), ART (Adaptive Resonance Theory), Boltzman machine, feature map, Hamming net, etc. However, a backpropagation neural network was chosen to solve our problem because it is most suitable for the pattern recognition application. It is also the simplest in architecture and implementation. It requires supervised training, which is relatively easy to implement.

Network Topology: The neural network was implemented on an HNC neurocomputing

92-32857



SP8

92 1 2 26 0 02

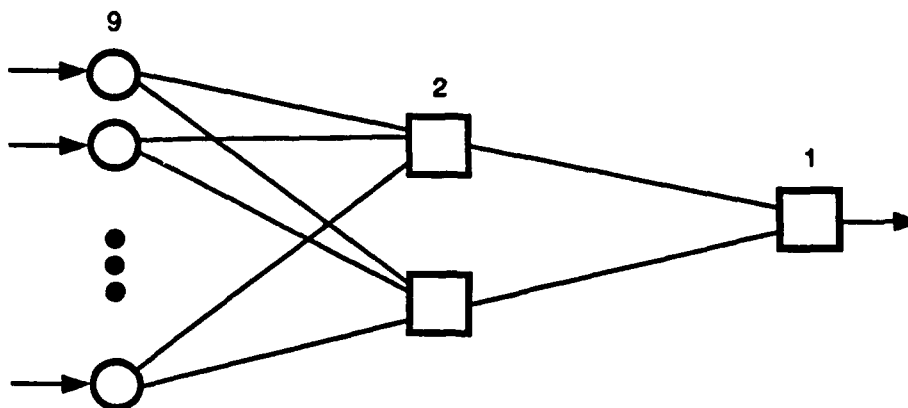


Figure 1. Network Configuration

coprocessor [2] interfaced with a SUN4 computer. It is a fully interconnected linkage of three layers as shown in Figure 1. The input layer consists of 9 PEs which are arranged to process a single pixel value simultaneously. Two PEs in a hidden layer are sufficient for delineating water from other terrain categories. A single PE with a thresholding function classified effectively all test images into two terrain categories: water and non-water.

Besides the input, hidden, and output layers, there are three auxiliary layers of PEs associated with this network. These auxiliary layers of PEs are automatically provided by the neurocomputer for the purposes of facilitating network training and performance once the main topology is determined. These auxiliary layers are not shown in Figure 1 for simplicity, however, they are briefly introduced below. A training layer is connected to the output layer in a one-to-one manner. This necessitates that the number of PEs in both the training and output layers be the same. A bias layer containing a single PE with a constant state of 1.0 is connected to each hidden and output PE. There is also a layer which computes statistics on the network's performance. The PEs in the input layer serve only to distribute the inputs; they perform no computation. For this reason, they are shown as circles to distinguish them from the computing PEs, which are shown as squares in Figure 1. Each computing PE in both hidden and output layers performs two tasks: summing and activation. The first task computes a summation for all input signals feeding into the PE. Each input signal represents a product of the output signal from the previous layer PE multiplied by its corresponding weight. A sigmoid activation function is applied to this summed signal to produce an output signal for this computing PE, thus completing the second task.

**Network Implementation:** The software for this backpropagation neural network was written by using the C language and the vendor supplied User Interface Subroutine Library (UISL), and was successfully implemented onto the neurocomputer described earlier. A switch was provided so that the network can be operated either in a training mode or in a classification mode. In the training mode, all 20 weights (18 weights between the input and hidden layers, and 2 weights between the hidden and output layers) are displayed on the screen of the SUN4 computer, and their changes can be observed and examined in real time. Two indicators were also provided to show the instantaneous changes of Mean Squared Error (MSE) and Mean Absolute Error (MAE) for the network during training. Memory is assigned to save the learned weights once the network training is successfully completed, and the satisfactory MSE and MAE are obtained. In the classification mode, a block

diagram illustrating the fully connected three-layered backpropagation neural network configuration (see Figure 1) is displayed. The input pixel value feeding an input PE is shown to the left side of each input PE, while the corresponding classified output value (either water:183 or non-water:0) is displayed on the right side of the output PE.

#### NETWORK TRAINING AND CLASSIFICATION RESULTS

**Network Training:** The training of the neural network was accomplished by using a block of 1,024 water pixels extracted from a water region of the first test image (Figure 2a). Each training pixel was sequentially fed into the network, and the MSE and MAE were automatically adjusted until the network converged. For our case, the MSE decreased very rapidly from approximately 0.5 to 0.00007 in less than 5 minutes. Originally, it was planned to use the same training set for classifying all test SAR images. However, it was discovered that the network poorly classified another SAR image (Figure 3a) having much brighter water regions (higher pixel values). This problem was solved by extracting another training set, having 1,024 pixels, from a water region of the second image and retrained the neural network.

**Network Classification and Results:** Two large-scale SAR images taken from the Elizabeth City, North Carolina area were used as test images for evaluating the classification accuracy of this backpropagation neural network. Each image consists of 512 by 512 pixels, and each pixel was digitized into 8 bits. These test images are shown in Figures 2a and 3a. A gray value of 183 was assigned as a water pixel, while a 0 gray value a non-water pixel. The first original SAR image, shown in Figure 2a, contains a large water body on its right side. The left side of the image consists mainly of fields, forests, and a built-up area. The classification results for this image are illustrated in Figure 2b. As seen in Figure 2b all water pixels were correctly classified. More than 99 percent of the non-water pixels were classified correctly. The misclassified non-water pixels belong to forest shadow regions which have pixel values similar to that of water pixels (in between 40 and 60). The second original image, shown in Figure 3a, consists of two large water bodies which are divided by a peninsula, and several small lakes located on the lower right part of the image. The land part of the image consists mainly of fields and forests. Similar classification results were obtained for this SAR image as shown in Figure 3b. Except for several water pixels on the top middle part of the image, all water pixels were correctly classified. The non-water pixels were again classified more than 99 percent correct. For the second image, the misclassified non-water pixels mainly belong to forest shadows and a small section of a road which is adjacent to the bottom of the image.

#### CONCLUSIONS

1. The classification of water pixels from SAR imagery using a backpropagation neural network appears to be quite interesting and useful.
2. A high classification accuracy can be obtained with a backpropagation neural network using only three computing PEs.

#### REFERENCES

- [1] Chen, P. F. and Tran, T. C., "Automated Water Finders for Radar Imagery," presented at the XVII International Society for Photogrammetry and Remote Sensing Congress, Washington, DC, August 1992.
- [2] Product Specification for "Balboa 860," HNC, Inc. 1991.

DEC

PAGE 2

1	2	3
4	5	6
7	8	9
10	11	12
13	14	15
16	17	18
19	20	21
22	23	24
25	26	27
28	29	30
31	32	33
34	35	36
37	38	39
40	41	42
43	44	45
46	47	48
49	50	51
52	53	54
55	56	57
58	59	60
61	62	63
64	65	66
67	68	69
70	71	72
73	74	75
76	77	78
79	80	81
82	83	84
85	86	87
88	89	90
91	92	93
94	95	96
97	98	99
100	101	102
103	104	105
106	107	108
109	110	111
112	113	114
115	116	117
118	119	120
121	122	123
124	125	126
127	128	129
130	131	132
133	134	135
136	137	138
139	140	141
142	143	144
145	146	147
148	149	150
151	152	153
154	155	156
157	158	159
160	161	162
163	164	165
166	167	168
169	170	171
172	173	174
175	176	177
178	179	180
181	182	183
184	185	186
187	188	189
190	191	192
193	194	195
196	197	198
199	200	201
202	203	204
205	206	207
208	209	210
211	212	213
214	215	216
217	218	219
220	221	222
223	224	225
226	227	228
229	230	231
232	233	234
235	236	237
238	239	240
241	242	243
244	245	246
247	248	249
250	251	252
253	254	255
256	257	258
259	260	261
262	263	264
265	266	267
268	269	270
271	272	273
274	275	276
277	278	279
280	281	282
283	284	285
286	287	288
289	290	291
292	293	294
295	296	297
298	299	300
301	302	303
304	305	306
307	308	309
310	311	312
313	314	315
316	317	318
319	320	321
322	323	324
325	326	327
328	329	330
331	332	333
334	335	336
337	338	339
340	341	342
343	344	345
346	347	348
349	350	351
352	353	354
355	356	357
358	359	360
361	362	363
364	365	366
367	368	369
370	371	372
373	374	375
376	377	378
379	380	381
382	383	384
385	386	387
388	389	390
391	392	393
394	395	396
397	398	399
400	401	402
403	404	405
406	407	408
409	410	411
412	413	414
415	416	417
418	419	420
421	422	423
424	425	426
427	428	429
430	431	432
433	434	435
436	437	438
439	440	441
442	443	444
445	446	447
448	449	450
451	452	453
454	455	456
457	458	459
460	461	462
463	464	465
466	467	468
469	470	471
472	473	474
475	476	477
478	479	480
481	482	483
484	485	486
487	488	489
490	491	492
493	494	495
496	497	498
499	500	501
502	503	504
505	506	507
508	509	510
511	512	513
514	515	516
517	518	519
520	521	522
523	524	525
526	527	528
529	530	531
532	533	534
535	536	537
538	539	540
541	542	543
544	545	546
547	548	549
550	551	552
553	554	555
556	557	558
559	560	561
562	563	564
565	566	567
568	569	570
571	572	573
574	575	576
577	578	579
580	581	582
583	584	585
586	587	588
589	590	591
592	593	594
595	596	597
598	599	600
601	602	603
604	605	606
607	608	609
610	611	612
613	614	615
616	617	618
619	620	621
622	623	624
625	626	627
628	629	630
631	632	633
634	635	636
637	638	639
640	641	642
643	644	645
646	647	648
649	650	651
652	653	654
655	656	657
658	659	660
661	662	663
664	665	666
667	668	669
670	671	672
673	674	675
676	677	678
679	680	681
682	683	684
685	686	687
688	689	690
691	692	693
694	695	696
697	698	699
700	701	702
703	704	705
706	707	708
709	710	711
712	713	714
715	716	717
718	719	720
721	722	723
724	725	726
727	728	729
730	731	732
733	734	735
736	737	738
739	740	741
742	743	744
745	746	747
748	749	750
751	752	753
754	755	756
757	758	759
760	761	762
763	764	765
766	767	768
769	770	771
772	773	774
775	776	777
778	779	780
781	782	783
784	785	786
787	788	789
790	791	792
793	794	795
796	797	798
799	800	801
802	803	804
805	806	807
808	809	810
811	812	813
814	815	816
817	818	819
820	821	822
823	824	825
826	827	828
829	830	831
832	833	834
835	836	837
838	839	840
841	842	843
844	845	846
847	848	849
850	851	852
853	854	855
856	857	858
859	860	861
862	863	864
865	866	867
868	869	870
871	872	873
874	875	876
877	878	879
880	881	882
883	884	885
886	887	888
889	890	891
892	893	894
895	896	897
898	899	900
901	902	903
904	905	906
907	908	909
910	911	912
913	914	915
916	917	918
919	920	921
922	923	924
925	926	927
928	929	930
931	932	933
934	935	936
937	938	939
940	941	942
943	944	945
946	947	948
949	950	951
952	953	954
955	956	957
958	959	960
961	962	963
964	965	966
967	968	969
970	971	972
973	974	975
976	977	978
979	980	981
982	983	984
985	986	987
988	989	990
991	992	993
994	995	996
997	998	999
1000	1001	1002



Figure 2a. First SAR Test Image

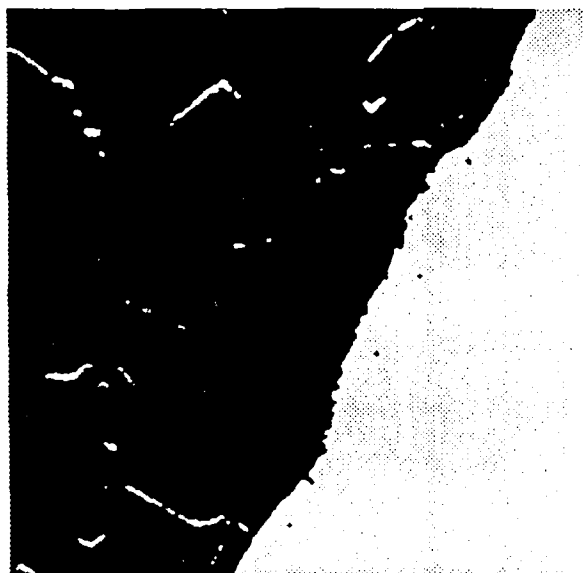


Figure 2b. Classified Results for The First SAR Test Image



Figure 3a. Second SAR Test Image



Figure 3b. Classified Results for The Second SAR Test Image